Int J Thermophys (2010) 31:276–296
DOI 10.1007/s10765-009-0699-7

# Review of the Thermodynamic Properties of Hydrogen Based on Existing Equations of State

**N. Sakoda · K. Shindo · K. Shinzato · M. Kohno · Y. Takata · M. Fujii**

Received: 15 May 2009 / Accepted: 30 December 2009 / Published online: 16 January 2010


**Abstract** Currently available equations of state (EOSs) for hydrogen are reviewed, and the data for the critical point, normal boiling point, and triple point are summarized. Through comparisons of PVT, saturated properties, heat capacity, and speed of sound among the latest EOSs for hydrogen, their features are discussed. The proper use of the EOSs, including a consideration of the nuclear isomers (ortho- and parahydrogen), is of great importance, especially for saturated properties, heat capacity, and speed of sound because these properties are different between the nuclear isomers. The present review concludes with recommendations for use of the EOSs for hydrogen.

**Keywords** Equation of state · Hydrogen · Review · Thermodynamic properties

## 1 Introduction

Hydrogen energy is expected to be a next-generation clean energy. For the development of hydrogen industries, accurate thermodynamic properties of hydrogen are essential. Systematic studies of the thermodynamic properties of hydrogen were made by the NIST (NBS)-NASA group in the low-temperature region, from 14 K to 300 K including the liquid phase (mainly for the space program) in the 1970s. In addition

N. Sakoda (✉)
Hydrogen Technology Research Center, Kyushu University, Fukuoka, Japan
e-mail: sakoda@mech.kyushu-u.ac.jp

K. Shindo · M. Kohno · Y. Takata
Department of Mechanical Engineering, Kyushu University, Fukuoka, Japan

K. Shinzato · M. Fujii
Research Center for Hydrogen Industrial Use and Storage (HYDROGENIUS), National Institute of Advanced Industrial Science and Technology (AIST), Fukuoka, Japan

to many experimental data, several equations of state (EOSs) for hydrogen have been published. In the low- and middle-temperature region from 98 K to 423 K, the van der Waals Laboratory group measured many PVT data in 1941 and 1959 [1,2]. Younglove [3] developed an EOS for parahydrogen based on these studies in 1982, and this EOS has been widely used. Since the release of Younglove's EOS, systematic PVT data in the temperature range from 273 K to 353 K and at pressures up to 28 MPa [4] were measured in 1990. Moreover, speed-of-sound data in the extremely high-pressure region from 1190 MPa to 10840 MPa in the temperature range from 293 K to 526 K [5], which is very close to the solid phase, were measured in 2003. Recently, the University of Idaho-NIST group studied the thermodynamic properties as well as the transport properties of hydrogen. Jacobsen et al. [6] summarized the existing measurements of the thermodynamic properties of hydrogen, and Leachman et al. [7] summarized the existing measurements of the transport properties of hydrogen. In addition, Leachman [8] developed three Helmholtz-type EOSs for ortho-, para-, and normal hydrogen compiling the existing measured data. These equations are also published in Leachman et al. [9]. In 2004, Kunz et al. [10] also developed a Helmholtz-type EOS for normal hydrogen as one of the components of natural gas, which is part of the GERG-2004 mixture model. Their results were published as a Technical Monograph [10] in 2007. Although these new EOSs have been developed very recently, no new measurements have been reported. In Japan, the Research Center for Hydrogen Industrial Use and Storage (HYDROGENIUS) was established in 2006 as a part of the National Institute of Advanced Industrial Science and Technology (AIST). It has constructed new research facilities specially designed for high-pressure hydrogen experiments up to 100 MPa, and some measurements have just been started [11].

Although a number of previous studies of the EOS for hydrogen have been published, their features need further clarification, and it is definitely of great importance to summarize them. Thus, currently available EOSs for hydrogen are reviewed in the present paper with comparisons of PVT, saturated properties, heat capacity, and speed of sound. Moreover, the important points of state, namely, the critical point, normal boiling point, and triple point, are also summarized, because their values are slightly different among the references, and it is sometimes confusing for users to choose appropriate values for them.

## 2 Existing Equations of State for Hydrogen

We compiled the studies of the EOS for hydrogen in Table 1, in which some articles that survey the thermodynamic properties of hydrogen in detail are also included. These studies contain thermodynamic property tables over wide temperature and pressure ranges that are very useful for easily obtaining approximate values of the thermodynamic properties. In Table 1, the EOS type is indicated with its available temperature and pressure ranges.

Hydrogen is classified into two isomers by the direction of the nuclear spin of the two atoms [24]. They are orthohydrogen and parahydrogen. The equilibrium composition of orthohydrogen and parahydrogen varies with temperature. At room temperature and above, hydrogen has a composition of 75 % orthohydrogen and 25 % parahydrogen,

**Table 1** Studies of equations of state for hydrogen

| Reference | Isomers of hydrogen | Equation type | Available range of EOS or tables | |
|---|---|---|---|---|
| | | | Temperature range (K) | Maximum Pressure (MPa) |
| Woolley et al. [12] | Normal | Polynomials EOS | 16–600 | 170 |
| Michels et al. [13] | Normal | Thermodynamic properties tables | 98–423 | 253 |
| Roder et al. [14] | Para | Polynomials EOS | 14–100 | 34 |
| McCarty and Weber [15] | Para | Polynomials EOS (16 terms) | 14–2778 | 69 |
| Roder et al. [16] | Para and equilibrium | Polynomials EOS (16 terms) | 14–3300 | 34 |
| McCarty [17] | Para | mBWR-type EOS (32 terms) | 14–2500 | 69 |
| Weber [18] | Para | Polynomials EOS | 14–300 | 100 |
| Roder and McCarty [19] | Para | mBWR-type EOS (32 terms) | 14–700 | 304 |
| McCarty [20] | Para and normal | Thermodynamic properties tables | 14–3000 | 100 |
| McCarty [21] | Ortho, para, and normal | mBWR-type EOS (32 terms) | 14–400 | 120 |
| McCarty et al. [22] | Para and normal | Thermodynamic properties tables | 14–3000 | 100 |
| Bender [23] | Normal | mBWR-type EOS (19 terms) | 18–700 | 50 |
| Younglove [3] | Para | mBWR-type EOS (32 terms) | 14–400 | 121 |
| Kunz et al. [10] | Normal | Helmholtz-type EOS (14 terms) | 14–700 | 300 |
| Leachman [8] | Ortho, para, and normal | Helmholtz-type EOS (14 terms) | 14–1000 | 2000 |

and the hydrogen with this composition is called normal hydrogen at all temperatures. The abundance ratio of parahydrogen in equilibrium increases with decreasing temperature, and below the normal boiling point, the ratio becomes 99.8 %. Equilibrium hydrogen designates hydrogen with equilibrium state compositions corresponding to a specified temperature. The conversion from orthohydrogen to parahydrogen is very slow, and at low temperatures around the normal boiling point, it takes more than a year to reach equilibrium hydrogen in the absence of paramagnetic catalysts [25]. Hence, parahydrogen and normal hydrogen are handled in practical cases, and the thermodynamic properties of parahydrogen and normal hydrogen are often discussed separately. Orthohydrogen does not exist as pure fluid (maximum composition of orthohydrogen is 75 %). Therefore, an EOS of orthohydrogen can only be estimated from a mixing rule for the isomers, parahydrogen and orthohydrogen. The result cannot be verified with experimental data. The difference between the thermodynamic properties of parahydrogen and normal hydrogen becomes appreciable for caloric properties such as heat capacity, speed of sound, enthalpy, and entropy. Differences

are observed also for the critical point and saturated properties, but little difference is apparent for other regions of the PVT surface.

Goodwin et al. [26] measured over 1200 points of PVT data from 15 K to 100 K and up to 35 MPa in 1963. The parahydrogen PVT surface was defined by these data, including the compressed liquid region. The thermodynamic properties of hydrogen before these data were surveyed by Woolley et al. [12]. They compiled PVT property tables in the gas phase only from 16 K to 600 K and up to 170 MPa. Michels et al. [13] compiled thermodynamic property tables from 98 K to 423 K and up to 253 MPa based on their own experimental PVT data [2].

After Goodwin measured his PVT data, several EOSs for hydrogen were developed, mainly by Roder, McCarty, and Weber from 1965 to 1981 as shown in Table 1. Among these, the EOS developed in 1975 by Roder and McCarty [19] for parahydrogen from 14 K to 700 K at pressures up to 304 MPa is notable. This EOS uses the modified Benedict–Webb–Rubin (mBWR) form and is able to represent the thermodynamic properties accurately in all fluid regions including gas, liquid, and supercritical fluid. Younglove [3] revised the EOS of Roder and McCarty by converting the unit of pressure from atmospheres to megapascals. Younglove reduced the application range to temperatures of 14 K to 400 K and a maximum pressure of 121 MPa. Especially the extrapolation of the EOS to higher pressures at elevated temperatures was questionable. The EOS of Younglove is expressed by

$$\begin{aligned} P = {} & \rho RT + \rho^2(N_1T + N_2T^{1/2} + N_3 + N_4/T + N_5/T^2) \\ & + \rho^3(N_6T + N_7 + N_8/T + N_9/T^2) \\ & + \rho^4(N_{10}T + N_{11} + N_{12}/T) + \rho^5(N_{13}) \\ & + \rho^6(N_{14}/T + N_{15}/T^2) + \rho^7(N_{16}/T) \\ & + \rho^8(N_{17}/T + N_{18}/T^2) + \rho^9(N_{19}/T^2) \\ & + \rho^3(N_{20}/T^2 + N_{21}/T^3)\exp(\gamma\rho^2) \\ & + \rho^5(N_{22}/T^2 + N_{23}/T^4)\exp(\gamma\rho^2) \\ & + \rho^7(N_{24}/T^2 + N_{25}/T^3)\exp(\gamma\rho^2) \\ & + \rho^9(N_{26}/T^2 + N_{27}/T^4)\exp(\gamma\rho^2) \\ & + \rho^{11}(N_{28}/T^2 + N_{29}/T^3)\exp(\gamma\rho^2) \\ & + \rho^{13}(N_{30}/T^2 + N_{31}/T^3 + N_{32}/T^4)\exp(\gamma\rho^2) \end{aligned} \tag{1}$$

where $P$ is the pressure, $\rho$ is the density, $R$ is the universal gas constant, and $T$ is the temperature. $N_i$ and $\gamma$ are empirically fitted coefficients.

Recently, accurate EOSs have been developed in the form of Helmholtz free energy functions. Kunz et al. [10] developed a Helmholtz-type EOS for natural gas (as a fluid mixture) by combining EOSs for pure components with mixing rules. The EOS of normal hydrogen is expressed as one of the components of natural gas, as follows:

$$a(\rho, T)/RT = \alpha^0(\delta, \tau) + \alpha^{\mathrm{r}}(\delta, \tau) \tag{2}$$

$$\alpha^0(\delta,\tau) = \frac{R^*}{R}\left[c^{\mathrm{II}} + c^{\mathrm{I}}\tau + c_0\ln(\tau) + \sum_{k=1,3} m_k \ln|\sinh(\theta_k\tau)| - \sum_{k=2,4} m_k \ln|\cosh(\theta_k\tau)| + \ln(\delta)\right] \tag{3}$$

$$\alpha^{\mathrm{r}}(\delta,\tau) = \sum_{i=1}^{5} n_i \delta^{d_i}\tau^{t_i} + \sum_{i=6}^{14} n_i \delta^{d_i}\tau^{t_i}\exp(-\delta^{p_i}) \tag{4}$$

where $a$ is the Helmholtz free energy. $R^*$ is the former universal gas constant ($= 8.314510\,\mathrm{J\cdot mol^{-1}\cdot K^{-1}}$), and $R$ is the presently accepted value of the universal gas constant ($= 8.314472\,\mathrm{J\cdot mol^{-1}\cdot K^{-1}}$). $\rho$, $T$, and $\alpha$ are the density, the temperature, and the dimensionless Helmholtz free energy, respectively. Superscript 0 denotes the ideal-gas part and r the residual part. $\alpha^{\mathrm{r}}$ has 14 terms. $\rho_{\mathrm{c}}$ and $T_{\mathrm{c}}$ are the critical density and critical temperature, respectively. $\delta = \rho/\rho_{\mathrm{c}}$, $\tau = T_{\mathrm{c}}/T$, and $c^{\mathrm{I}}$, $c^{\mathrm{II}}$, $c_0$, $m_k$, and $\theta_k$ are the coefficients of the ideal-gas part of the dimensionless Helmholtz free energy. This ideal-gas part is based on an expression for the ideal-gas specific heat capacity as given by Eq. 5 but has different values for the coefficients. $n_i$, $d_i$, $t_i$, and $p_i$ are the coefficients of the residual part of the dimensionless Helmholtz free energy. The available range of Eqs. 2–4 is from 14 K to 700 K and up to 300 MPa.

Leachman [8] developed three Helmholtz-type EOSs for ortho-, para-, and normal hydrogen. The expression of the EOSs is the same as Eq. 2, although the ideal-gas specific heat capacity is expressed by Eq. 5. The Helmholtz free energy of the ideal gas is derived from the ideal-gas specific heat capacity by thermodynamic relations. The residual part given by Eq. 6 has 14 terms, and the number of terms is the same as that of Kunz et al., although the expression is different. The EOSs of Leachman contain Gaussian terms that can express the features well in the region close to the critical point.

$$\frac{C_P^0}{R} = n_0 + \sum_k v_k \left(\frac{u_k}{T}\right)^2 \frac{\exp(u_k/T)}{[\exp(u_k/T)-1]^2} \tag{5}$$

$$\alpha^{\mathrm{r}}(\delta,\tau) = \sum_{i=1}^{7} n_i \delta^{d_i}\tau^{t_i} + \sum_{i=8}^{9} n_i \delta^{d_i}\tau^{t_i}\exp(-\delta^{p_i}) + \sum_{i=10}^{14} n_i \delta^{d_i}\tau^{t_i}\exp[\varphi_i(\delta - D_i)^2 + \beta_i(\tau-\gamma_i)^2] \tag{6}$$

where $C_P^0$ is the ideal-gas specific heat capacity and $n_0$, $v_k$, $u_k$, $n_i$, $d_i$, $t_i$, $p_i$, $\varphi_i$, $D_i$, $\beta_i$, and $\gamma_i$ are the coefficients. The coefficients for the three EOSs corresponding to ortho-, para-, and normal hydrogen are different from each other. The experimental data are not sufficient for normal hydrogen, and there are no experimental data for orthohydrogen because it does not exist naturally in a pure state. Therefore, in the

process of developing these EOSs, the data for parahydrogen were converted to normal hydrogen or orthohydrogen by considering their intermolecular forces.

## 3 Uncertainties of the Equations of State

For the proper use of the EOSs, estimation of uncertainties is very important, and it is desirable that the estimation should be performed based on comparisons with experimental data having definite uncertainties. However, some studies reporting experimental data do not mention their uncertainties. Therefore, the uncertainties of the EOSs are often estimated based solely on deviations from the experimental data. Some of the EOSs in Table 1 mentioned their uncertainties. Figure 1 shows the density uncertainties derived from three EOSs, i.e., McCarty and Weber [15], Younglove [3], and Leachman [8]. The uncertainties were estimated based on the deviations from the experimental data.

The density uncertainties for the EOS of McCarty and Weber shown in Fig. 1a are 0.1 % below 100 K and 0.5 % from 100 K to 700 K. The specified region of applicability of this EOS is larger than the region in which experimental data are available. The uncertainty in the extrapolation regions is 1 %. The uncertainty of the derived properties, such as isobaric and isochoric heat capacity, speed of sound, enthalpy, entropy, and internal energy, is estimated to be 2 % below 100 K, and it is estimated

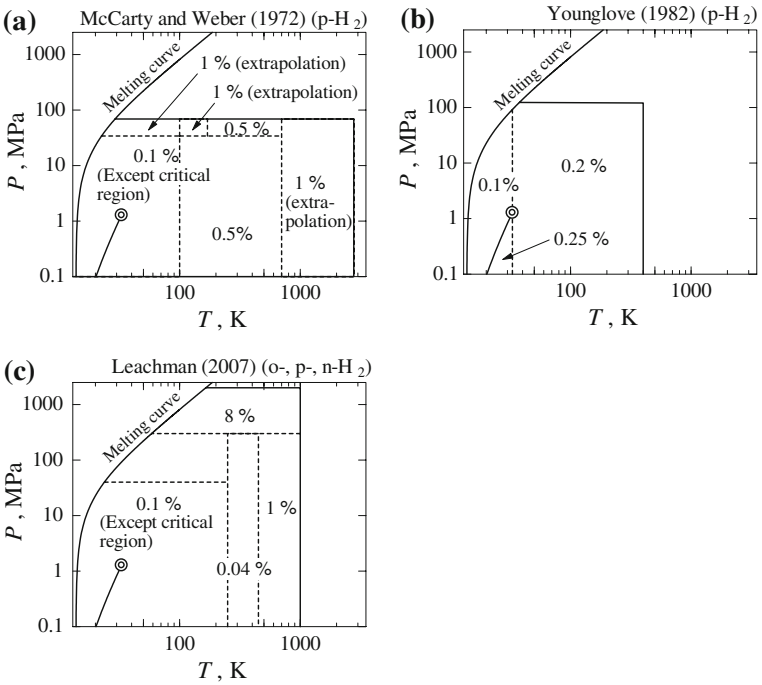


**Fig. 1** Density uncertainties of **(a)** McCarty and Weber [15], (**b**) Younglove [3], and **(c)** Leachman [8]: ( ◎ ) critical point; $o$-$H_2$: orthohydrogen, $p$-$H_2$: parahydrogen, $n$-$H_2$: normal hydrogen

to be 10 % in the extrapolation region below 100 K. The uncertainties are estimated to be 2 % from 100 K to 700 K and up to 35 MPa and 5 % from 700 K to 3000 K. For the derived property calculations, the ideal-gas heat capacity equation of Woolley et al. [12] was used, and its uncertainty is estimated to be 0.3 %.

The density uncertainty of the EOS of Younglove is shown in Fig. 1b. Below the critical temperature, the uncertainty in the gas phase is 0.25 % and that in the liquid phase is 0.1 %. From the critical temperature to 400 K and up to 121 MPa, the uncertainty is 0.2 %. Moreover, for the fluid region above the critical temperature, the uncertainties of heat capacity, speed of sound, and enthalpy are 3.0 %, 1.0 %, and 5.1 $J \cdot mol^{-1}$, respectively. The uncertainty of entropy is 1.0 %.

The density uncertainty of the EOS of Leachman is shown in Fig. 1c. He also estimated the uncertainties based on deviations from experimental data. The uncertainties of ortho-, para-, and normal hydrogen are estimated to be almost the same. The uncertainty is smaller compared with the EOS of Younglove because of the improvement in the fitting technique. The uncertainty of the speed of sound below 100 MPa is 0.5 %, and that of the specific heat capacity is estimated to be 1.0 %. The uncertainties for vapor pressure and saturated liquid density are estimated to be 0.1 % for parahydrogen and 0.2 % for normal hydrogen.

## 4 Specific Points of State

The critical point, normal boiling point, and triple point are fixed-point properties which roughly characterize the behavior of fluids. These values for hydrogen are summarized in Tables 2, 3, and 4.

The critical points are different for parahydrogen and normal hydrogen. White et al. [27] determined the critical temperature and critical pressure of normal hydrogen from observation of the disappearance of the meniscus between the vapor and liquid. However, almost all the reported critical points were determined analytically. Roder and McCarty [19] determined the critical point of parahydrogen by the rectilinear diameter method from the saturated density of Roder et al. [29]. Leachman [8] allowed the critical point to float in the fitting procedure. The resulting value of the critical point agrees closely with values predicted by the rectilinear diameter method. The critical points of normal hydrogen and orthohydrogen were determined through correlation of the transformed saturated properties and PVT near the critical point in the process of developing the EOSs. For the present, it is recommended to use the critical points of parahydrogen and normal hydrogen of Leachman from the point of view of consistency with the saturated properties and PVT. However, the difference of the critical densities between parahydrogen and normal hydrogen reaches 4 %, and hence accurate measurements are needed to verify this difference.

The normal boiling-point temperature is often calculated from an EOS or a saturated vapor-pressure equation at 0.101 325 MPa. Roder and McCarty determined the normal boiling point of parahydrogen as 20.277 K from the saturated vapor-pressure equation. McCarty [21] calculated the normal boiling points of parahydrogen and normal hydrogen from the mBWR-type EOS of Roder and McCarty. He developed a computer program to calculate the thermodynamic properties of ortho-, para-, and normal

**Table 2** Summary of values for the critical point of hydrogen

| Reference | Isomers of hydrogen | $T_c$ (K) | $P_c$ (MPa) | $\rho_c$ (mol · dm$^{-3}$) | Remarks |
|---|---|---|---|---|---|
| Woolley et al. [12][c] | Normal | 33.19 | 1.315 (12.98 atm)[a] | 14.94 ($v_c = 66.95$ cm$^3$ · mol$^{-1}$)[a] | Determined from PVT and saturated properties |
| White et al. [27] | Normal | 33.244 | 1.2967 (12.797 atm)[a] | – | Determined from the disappearance of the meniscus between vapor and liquid |
| Hoge and Lassiter [28] | Para | 32.994 | 1.2939 (12.770 atm)[a] | 15.27 ($v_c = 65.5$ cm$^3$ · mol$^{-1}$)[a] | Determined from PVT |
| Roder et al. [29] | Para | 32.976 | 1.2928 (12.759 atm)[a] | 15.59 | Determined from PVT and saturated properties |
| Roder et al. [14][c] | Para | 32.976 | 1.2928 (12.759 atm)[a] | 15.59 | Adopted from Roder et al. [29] |
| McCarty and Weber [15][c] | Para | 32.976 | 1.2928 (12.759 atm)[a] | 15.59 | Cited in the appendix |
| Roder et al. [16][c] | Para | 32.976 (59.356 R) | 1.2928 (187.506 psia)[a] | – | – |
| McCarty [17][c] | Para | 32.938 | 1.2838 (12.670 atm)[a] | 15.556 | Determined by the rectilinear diameter method |
| Weber [18][c] | Para | 32.976 | 1.2928 | 15.59 | Adopted from Roder et al. [14] |
| Roder and McCarty [19][c] | Para | 32.938 | 1.2838 (12.670 atm)[a] | 15.556 | Determined by the rectilinear diameter method |
| McCarty [20][c] | Para | 32.976 | 1.2928 | 15.59 | Adopted from Roder et al. [14] |
| McCarty [20][c] | Normal | 33.19 | 1.315 | 14.94 | Adopted from Woolley et al. [12] |
| McCarty [21][c] | Para | 32.938 | 1.283768 | 15.556 | – |
| McCarty et al. [22][c] | Para | 32.976 | 1.2928 | 15.59 | Adopted from Roder et al. [14] |
| McCarty et al. [22][c] | Normal | 33.19 | 1.315 | 14.94 | Adopted from Woolley et al. [12] |
| Younglove [3][c] | Para | 32.938 | 1.28377 | 15.556 | Adopted from Roder and McCarty [19] |
| Kunz et al. [10][c] | Normal | 33.19 | 1.315[b] | 14.94 | – |

**Table 2** continued

| Reference | Isomers of hydrogen | $T_c$ (K) | $P_c$ (MPa) | $\rho_c$ (mol·dm$^{-3}$) | Remarks |
|---|---|---|---|---|---|
| Leachman [8][c] | Para | 32.938 | 1.2858 | 15.538 | Determined through correlation of the saturated properties and PVT near the critical point |
| Leachman [8][c] | Normal | 33.145 | 1.2964 | 15.508 | Determined through correlation of the saturated properties and PVT near the critical point |
| Leachman [8][c] | Ortho | 33.22 | 1.31065 | 15.445 | Determined through correlation of the saturated properties and PVT near the critical point |

[a] Original value in the reference
[b] Calculated value from the EOS in the present work
[c] Reference shown in Table 1

hydrogen [21]. Although PVT is calculated by the mBWR-type EOS, heat property calculations require an additional ideal-gas heat-capacity equation. In his calculations, the mBWR-type EOS was commonly used and an ideal-gas heat-capacity equation was changed corresponding to ortho-, para-, and normal hydrogen, because that property differs between the nuclear isomers. The normal boiling point is calculated by the mBWR-type EOS without using the ideal-gas heat-capacity equation. Therefore, the same values of the normal boiling points of ortho-, para-, and normal hydrogen are calculated and cited in the reference of Roder and McCarty. Ancsin [37] carefully measured the normal boiling points and the triple points of parahydrogen and normal hydrogen in 1977. Kemp and Kemp [38] also carefully measured the triple point and normal boiling point of parahydrogen, and these data were chosen as primary data for the EOS of Leachman for parahydrogen. The latest experimental data of the saturated vapor pressure were measured by Hiza [39] for normal hydrogen from 20 K to 30 K in 1981. He also developed a saturated vapor-pressure equation and determined the normal boiling point of normal hydrogen from the equation. According to the International Temperature Scale of 1990 (ITS-90), the triple point of parahydrogen is defined as a fixed point, which is 13.8033 K. Bedford et al. [40], who were in a working group of the Comite Consultatif de Thermometrie (CCT), which is a committee of the Bureau International des Poids et Mesures (BIPM), mentioned the recommended value of the triple point of the normal hydrogen, and those of the normal boiling point of parahydrogen and normal hydrogen in 1996, and they referred to the values of Ancsin, which

**Table 3** Summary of values for the normal boiling point of hydrogen

| Reference | Parahydrogen | Normal hydrogen |
|---|---|---|
| | $T_{nbp}$ (K) | $T_{nbp}$ (K) |
| Keesom et al. [30] | 20.279 (−252.871 °C)[a] | 20.396 (−252.754 °C)[a] |
| Scott et al. [31] | – | 20.38 |
| Woolley et al. [12][c] | 20.273 | 20.390 |
| Hoge and Arnold [32] | 20.278 | – |
| Grilly [33] | – | 20.39 |
| Weber et al. [34] | 20.268 | – |
| Barber and Horsford [35] | 20.2705 | – |
| van Itterbeek et al. [36] | 20.269 | 20.389 |
| Roder et al. [14][c] | 20.268 | – |
| McCarty and Weber [15][c] | 20.268 | – |
| Roder et al. [16][c] | 20.268 (36.482 R)[a] | – |
| Weber [18][c] | 20.268 | – |
| Roder and McCarty [19][c] | 20.277 | – |
| McCarty [20][c] | 20.268 | 20.39 |
| Ancsin [37] | 20.28 | 20.397 |
| Kemp and Kemp [38] | 20.28 | |
| McCarty [21][c] | 20.27686 | 20.27686 |
| Hiza [39] | – | 20.375 |
| McCarty et al. [22][c] | 20.268 | 20.39 |
| Younglove [3][c] | 20.277[b] | – |
| Bedford et al. [40] | 20.271 | 20.388 |
| Kunz et al. [10][c] | – | 20.380[b] |
| Leachman [8][c] | 20.271[b] | 20.369[b] |

[a] Original value in the reference
[b] Calculated value from the EOS in the present work
[c] Reference shown in Table 1

were converted from the International Practical Temperature Scale of 1968 (IPTS-68) to ITS-90. These recommended values are also referenced by Goodwin et al. [42].

## 5 Comparisons Among the Latest Equations of State for Hydrogen

The EOS of Younglove [3] for parahydrogen has been widely used for thermodynamic property calculations. Recently, Kunz et al. [10] developed a Helmholtz-type EOS for normal hydrogen, and Leachman [8] developed three Helmholtz-type EOSs for ortho-, para-, and normal hydrogen. These Helmholtz-type EOSs cover a wide range of applications as shown in Table 1. The WebBook of NIST [43] has replaced the hydrogen EOS of Younglove [3] with that of Leachman [8]. Clarifying the features and the differences among these EOSs is of great importance as well as the differences in

**Table 4** Summary of values for the triple point of hydrogen

| Reference | Parahydrogen | | Normal hydrogen | |
|---|---|---|---|---|
| | $T_t$ (K) | $P_t$ (MPa) | $T_t$ (K) | $P_t$ (MPa) |
| Scott et al. [31] | – | – | 13.92 | 0.00720 (54 mmHg)[a] |
| Henning and Otto [41] | – | – | 13.96 | 0.00721 (54.1 mmHg)[a] |
| Woolley et al. [12][b] | 13.813 | 0.00704 (52.8 mmHg)[a] | 13.957 | 0.00720 (54.0 mmHg)[a] |
| Hoge and Arnold [32] | 13.813 | 0.00704 (52.8 mmHg)[a] | – | – |
| Grilly [33] | – | – | 13.96 | 0.00720 (54.0 mmHg)[a] |
| Barber and Horsford [35] | 13.816 | 0.00706 (52.95 mmHg)[a] | – | – |
| Roder et al. [14][b] | 13.803 | 0.00704 (0.0695 atm)[a] | – | – |
| McCarty and Weber [15][b] | 13.803 | 0.00704 (0.0695 atm)[a] | – | – |
| Roder et al. [16][b] | 13.803 (24.845 R) | 0.00705 (1.022 psia)[a] | – | – |
| McCarty [17][b] | 13.8 | 0.00704 (0.0695 atm)[a] | – | – |
| Weber [18][b] | 13.803 | 0.00704 | – | – |
| Roder and McCarty [19][b] | 13.8 | 0.00704 (0.0695 atm)[a] | – | – |
| McCarty [20][b] | 13.803 | 0.00704 | 13.957 | 0.00720 |
| Ancsin [37] | 13.81 | 0.0070345 | 13.958 | 0.0072103 |
| Kemp and Kemp [38] | 13.81 | – | – | – |
| McCarty [21][b] | 13.8 | 0.007043101 | – | – |
| McCarty et al. [22][b] | 13.803 | 0.00704 | 13.957 | 0.00720 |
| Younglove [3][b] | 13.8 | 0.007042 | – | – |
| Bedford et al. [40] | 13.8033 | – | 13.952 | – |
| Leachman [8][b] | 13.8033 | 0.007041 | 13.957 | 0.00736 |

[a] Original value in the reference
[b] Reference shown in Table 1

the properties among ortho-, para-, and normal hydrogen. The comparisons for PVT, saturated properties, isobaric heat capacity, and speed of sound are presented in this section.

## 5.1 PVT

The PVT surface calculated from the EOS of Leachman for parahydrogen is shown in Fig. 2 on the $P$–$\rho$–$T$ plane, where the temperature range is from the triple point of 13.8033 K to 800 K at pressures up to 100 MPa. In addition, some existing experimental data are also plotted in Fig. 2. Figure 3 shows the density deviations of the

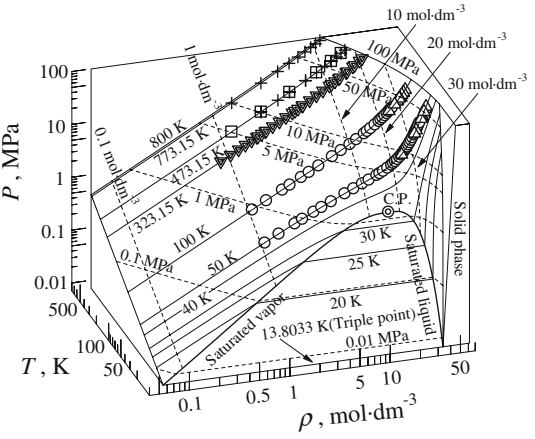


**Fig. 2** PVT surface calculated from the EOS of Leachman [8] for parahydrogen with some experimental data: ( □ ) Wiebe and Gaddy ($n$-$H_2$) [56], ( ▽ ) Michels et al. ($n$-$H_2$) [2], (◯) Goodwin et al. ($p$-$H_2$) [26], (Δ) Weber ($p$-$H_2$) [18], (+) Presnall ($n$-$H_2$) [48], ( ◎ ) critical point

experimental data, the EOS of Younglove that of Kunz et al. and those of Leachman for normal hydrogen and orthohydrogen from the EOS of Leachman for parahydrogen along isotherms at 50 K, 100 K, 323.15 K, 473.15 K, and 773.15 K. Temperatures of some experimental data in Fig. 3 are not exactly, but almost the same as these temperatures. It should be noted that the described vertical range at 50 K, 100 K, 323.15 K, and 473.15 K is ±0.5 %, but it is ±1 % at 773.15 K. The available range of the EOS of Younglove is from the triple point to 400 K and up to 121 MPa, and that of Kunz et al. is from the triple point to 700 K and up to 300 MPa as shown in Table 1, so Fig. 3 includes the extrapolated region for these EOSs. The EOS of Leachman for parahydrogen agrees with that of Younglove within ±0.2 % up to 45 MPa at temperatures of 50 K and 100 K although the deviations increase as pressure increases above 45 MPa. The deviations show 0.36 % at 50 K and 100 MPa, and 0.92 % at 100 K and 100 MPa. The EOS of Leachman for parahydrogen shows very good agreement with the data of Michels et al. [2] within ±0.05 % at 323.15 K up to 250 MPa. There are other high-pressure data of more than 100 MPa by Amagat [44] and Tsiklis et al. [45]. The EOS of Leachman for parahydrogen agrees well with the data of Tsiklis et al. Liebenberg et al. [46] measured extremely high pressure PVT data for normal hydrogen from 200 MPa to 2200 MPa in the temperature range from 75 K to 307 K, and they developed a polynomial-type EOS that is available for this temperature and pressure region [47] based on the measurements. The calculated values from the EOS of Liebenberg et al. show large deviations compared with the EOSs of Leachman, and for instance, at 100 K, the density deviations from the EOS of Leachman for normal hydrogen are −0.73 % at 200 MPa and −0.82 % at 500 MPa. When compared with experimental data, the EOS of Leachman for parahydrogen shows better agreement with the measurements of Michels et al., Goodwin et al. [26], and Weber [18] than that of Younglove. For the high-temperature region at 473.15 K and 773.15 K, the EOSs are in good agreement within ±0.2 % of each other up to 200 MPa except for the EOS of Younglove with its maximum pressure of 121 MPa. However, at 773.15 K, the only existing experimental data (Presnall [48]) show large deviations uniformly from the EOSs of Leachman and the other EOSs, and the

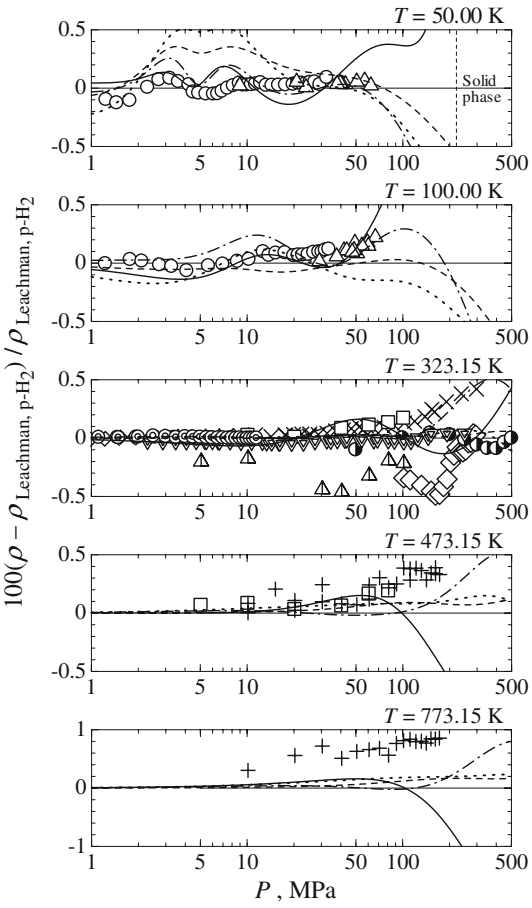


**Fig. 3** Deviations of density from the EOS of Leachman for parahydrogen [8]: (◇) Amagat ($n$-$H_2$) [44], (◭) Bartlett et al. ($n$-$H_2$) [57], (□) Wiebe and Gaddy ($n$-$H_2$) [56], (×) Michels and Goudeket ($n$-$H_2$) [1], (▽) Michels et al. ($n$-$H_2$) [2], (◯) Goodwin et al. ($p$-$H_2$) [26], (◑) Tsiklis et al. ($n$-$H_2$) [45], (Δ) Weber ($p$-$H_2$) [18], (+) Presnall ($n$-$H_2$) [48], (◎) Jaeschke and Humphreys ($n$-$H_2$) [4], (———) Younglove ($p$-$H_2$) [3], (— · — · —) Kunz et al. ($n$-$H_2$) [10], (– – – – –) Leachman ($n$-$H_2$) [8], (. . . . . .) Leachman ($o$-$H_2$) [8]

deviations reach 0.8 % at more than 100 MPa. There are few accurate experimental data at high temperatures above 473.15 K, and new measurements are highly desired in this region.

## 5.2 Vapor–Liquid Equilibrium

The deviations of the saturated vapor pressure from the EOSs of Leachman for parahydrogen and normal hydrogen are shown in Fig. 4. The baseline of Fig. 4a is the EOS of Leachman for parahydrogen, and that of Fig. 4b is the EOS of Leachman for normal hydrogen. The saturated properties are different among the nuclear isomers. The EOSs of Leachman for orthohydrogen and normal hydrogen deviate from −4.5 % to −2.2 % compared with the EOS of Leachman for parahydrogen. The EOS of Leachman for parahydrogen and that of Younglove agree with each other within 0.4 %. The EOS of Kunz et al. does not agree well with the experimental data of normal hydrogen and shows trends differently from that of Leachman for normal hydrogen in Fig. 4b. Figure 5a1

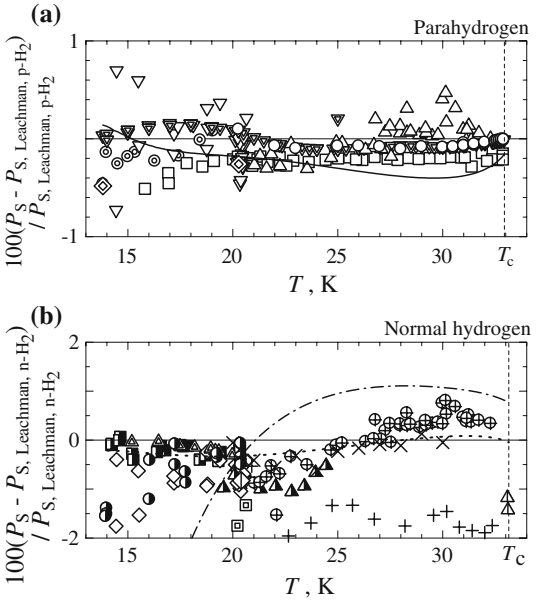


**Fig. 4** Deviations of saturated vapor pressure from the EOSs of Leachman for **(a)** parahydrogen and **(b)** normal hydrogen [8]: (▽) Keesom et al. ($p$-$H_2$) [30], (◇) Keesom et al. ($n$-$H_2$) [30], (◬) Scott et al. ($n$-$H_2$) [31], (▣) Aston et al. ($n$-$H_2$) [58], (◑) Henning and Otto ($n$-$H_2$) [41], (◧) Scott and Brickwedde ($n$-$H_2$) [59], (+) White et al. ($n$-$H_2$) [60], (◭) White et al. ($n$-$H_2$) [27], (□) Hoge and Arnold ($p$-$H_2$) [32], (◬) Grilly ($n$-$H_2$) [33], (◯) Weber et al. ($p$-$H_2$) [34], (◎) Barber and Horsford ($p$-$H_2$) [35], (▼) Roder et al. ($p$-$H_2$) [29], (△) van Itterbeek et al. ($p$-$H_2$) [36], (⊕) van Itterbeek et al. ($n$-$H_2$) [36], (◈) Ancsin ($p$-$H_2$) [37], (◈) Ancsin ($n$-$H_2$) [37], (×) Hiza ($n$-$H_2$) [39], (———) Younglove ($p$-$H_2$) [3], (— · — · —) Kunz et al. ($n$-$H_2$) [10], (. . . . . .) Leachman ($o$-$H_2$) [8]

and a2 shows deviations of the saturated liquid density from the EOSs of Leachman for parahydrogen and normal hydrogen, and Fig. 5b shows deviations of the saturated-vapor density from the EOS of Leachman for parahydrogen. The saturated liquid densities calculated from the EOSs of Younglove and Leachman are in good agreement except near the critical temperature, and they agree within 0.3 % below 30 K as shown in Fig. 5a1. The saturated liquid density calculated from the EOS of Leachman for normal hydrogen agrees with that of Leachman for orthohydrogen within 0.1 % except near the critical temperature in Fig. 5a2. The saturated-vapor density calculated from the EOS of Leachman for parahydrogen agrees with the measurements of Roder et al. [29] within ±0.2 % except near the critical point as shown in Fig. 5b. The saturated-vapor densities calculated from the EOSs of Leachman for orthohydrogen and normal hydrogen and that of Kunz et al. show large differences of more than 2.5 % from the EOS of Leachman for parahydrogen. These deviations are considered to be due to the difference among nuclear isomers. In order to verify the difference among nuclear isomers and estimate the uncertainty of the calculated saturated-vapor density from the EOSs, measurements of vapor–liquid equilibrium for normal hydrogen are essential.

The saturated-vapor-pressure and saturated-density measurements for parahydrogen by Roder et al. [29] have been the basic experimental data for developing the EOS. In addition, the saturated-vapor-pressure measurements for parahydrogen by Weber

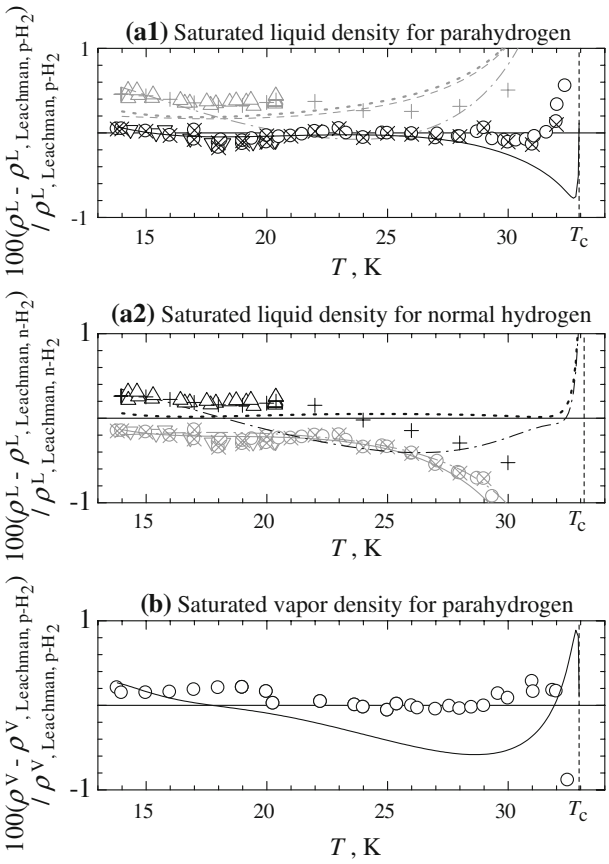


**Fig. 5** Deviations of saturated liquid and vapor density from the EOSs of Leachman [8]; **(a1)** saturated liquid density for parahydrogen, **(a2)** saturated liquid density for normal hydrogen, and **(b)** saturated vapor density for parahydrogen: (∇) Scott and Brickwedde ($p$-$H_2$) [59],(Δ) Scott and Brickwedde ($n$-$H_2$) [59], (×) Goodwin et al. ($p$-$H_2$) [49], (+) Goodwin et al. ($n$-$H_2$) [49], (◯) Roder et al. ($p$-$H_2$) [29], (———) Younglove ($p$-$H_2$) [3], (—·—·—) Kunz et al. ($n$-$H_2$) [10], (—··—) Leachman ($p$-$H_2$) [8], (– – – – –) Leachman ($n$-$H_2$) [8], (.....) Leachman ($o$-$H_2$) [8]

et al. [34] and the saturated-liquid-density measurements for parahydrogen and normal hydrogen by Goodwin et al. [49] have been used as primary experimental data. The EOSs of Leachman show better representation of these experimental data than does that of Younglove.

## 5.3 Isobaric Heat Capacity

The isobaric heat-capacity surface of parahydrogen calculated from the EOS of Leachman is shown in Fig. 6. The experimental data of Medvedev et al. [50] at 1.08 MPa and 3.04 MPa are also plotted in the figure. Medvedev et al. measured 320 points of the isobaric heat capacity data for the temperature range from 21 K to 50 K and the pressure range from 0.2 MPa to 3.0 MPa. For the isochoric heat capacity of hydrogen,

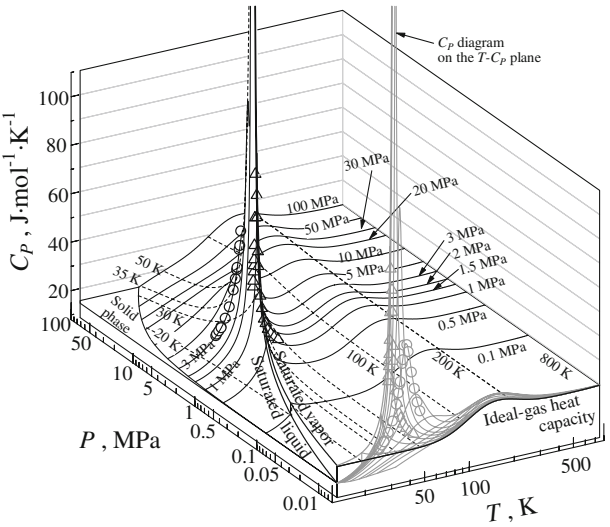


**Fig. 6** Isobaric heat capacity surface calculated from the EOS of Leachman [8] for parahydrogen with some experimental data: Δ Medvedev et al. ($p$-$H_2$, 1.08 MPa) [50], (○) Medvedev et al. ($p$-$H_2$, 3.04 MPa) [50]

there are only data by Younglove and Diller [51], which are 160 data points and cover the temperature range from 20 K to 90 K and the pressure range from 1 MPa to 63 MPa. Most of the region of the derived property surfaces such as isobaric and isochoric heat capacities relies on the calculations derived by the EOS that was developed based on PVT and speed-of-sound data. For hydrogen, the isobaric heat capacity of the saturated liquid is lower than that of the saturated vapor and the ideal-gas heat capacity as shown in Fig. 6, which is different from most other fluids. This tendency is also seen for the isochoric heat-capacity measurements of Younglove and Diller. However, the isochoric heat capacity of the saturated liquid calculated by the EOS of Kunz et al. is larger than that of the saturated vapor and the ideal-gas heat capacity, and this behavior does not represent the experimental data.

Figure 7a shows the isobaric ideal-gas heat capacities of ortho-, para-, and normal hydrogen calculated from the EOSs of Leachman, and Fig. 7b1 and b2 shows the deviations from the EOSs of Leachman for parahydrogen and normal hydrogen. The ideal-gas heat capacity is only a function of temperature. The maximum deviation among the nuclear isomers reaches approximately 30 % near 150 K. The ideal-gas heat capacities of the nuclear isomers calculated by Leachman agree with each other below 30 K. Figure 7b1 shows the ideal-gas heat-capacity deviations of the EOS of Younglove from the EOS of Leachman for parahydrogen, and Fig. 7b2 shows those of the EOS of Kunz et al. from the EOS of Leachman for normal hydrogen. The ideal-gas heat capacity of Younglove agrees with that of Leachman for parahydrogen within 0.1 % but the deviation above 400 K increases because this range is the extrapolated region for the EOS of Younglove. The ideal-gas heat capacity of Kunz et al. shows a 0.84 % deviation from that of Leachman even below 30 K because the EOS of Kunz

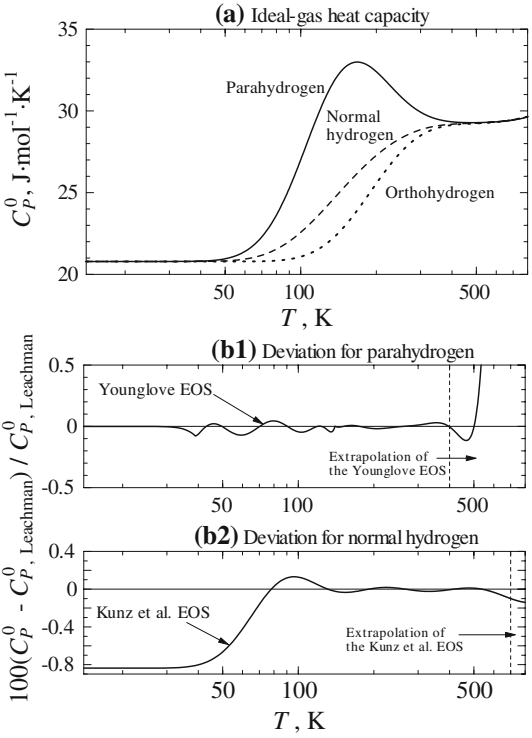


**Fig. 7** Comparisons with ideal-gas heat capacities of ortho-, para-, and normal hydrogen: **(a)** behavior of ideal-gas heat capacities calculated from the EOSs of Leachman [8] for ortho-, para-, and normal hydrogen, **(b1)** deviation of the ideal-gas heat capacity of Younglove [3] from the EOS of Leachman [8] for parahydrogen, and **(b2)** deviation of the ideal-gas heat capacity of Kunz et al. [10] from the EOS of Leachman [8] for normal hydrogen

et al. uses a correlation for ideal-gas heat capacities derived only for the temperature range from 100 K to 1000 K [52].

The comparisons of isobaric heat capacity with the EOSs of Leachman for parahydrogen and normal hydrogen are shown in Fig. 8. Figure 8a1 and a2 shows deviations of the experimental data of Medvedev et al. and the EOS of Younglove for parahydrogen. The baseline of these figures is the EOS of Leachman for parahydrogen. The EOS of Leachman for parahydrogen agrees with that of Younglove within ±0.6 % from 100 K to 400 K. Most of the experimental data agrees with the EOS of Leachman within ±1.5 % at 3 MPa, but the deviation reaches 5 % at 1 MPa. This region is near the critical point as shown in Fig. 6, and it is usually difficult to fit the EOS to experimental data in this region. The density deviation between the EOS of Younglove and that of Leachman for parahydrogen increases as pressure increases at 50 K and 100 K as shown in Fig. 3. At 50 K and 100 MPa, the density deviation and the isobaric-heat-capacity deviation of the EOS of Younglove from the EOS of Leachman for parahydrogen are +0.4 % and −5.1 %, respectively. However, at 100 K and 100 MPa, the density deviation is +0.9 % and the isobaric-heat-capacity deviation is −0.09 %. As experimental data at 50 K and 100 K are not available, it is desirable to have new measurements at low temperature and high pressure for isobaric heat capacities or speed of sound in order to resolve this disagreement. At 773.15 K, the isobaric heat capacities calculated by the EOSs agree well with each other as for the densities shown

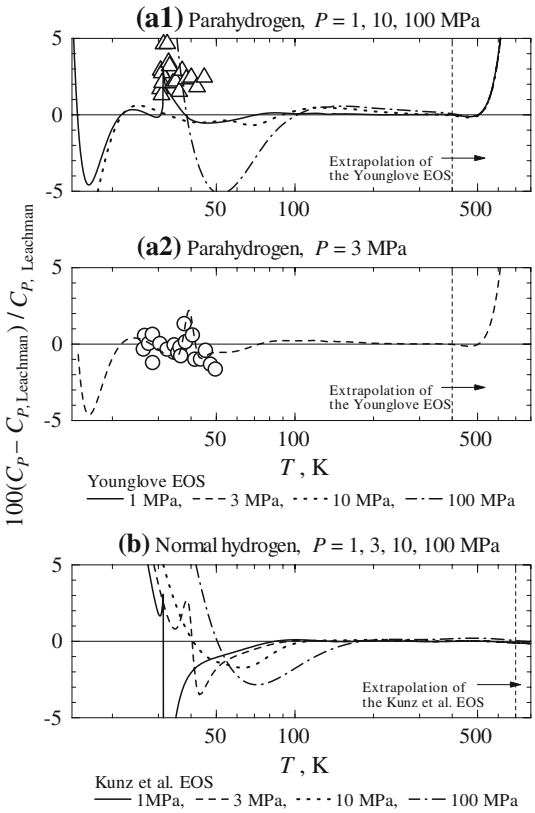


**Fig. 8** Deviations of isobaric heat capacity from the EOSs of Leachman [8] for parahydrogen and normal hydrogen, **(a1)** pressures are 1 MPa, 10 MPa, and 100 MPa for parahydrogen, **(a2)** pressure is 3 MPa for parahydrogen, and **(b)** pressures are 1 MPa, 3 MPa, 10 MPa, and 100 MPa for normal hydrogen: (△) Medvedev et al. ($p$-$H_2$, 1.08 MPa) [50], (○) Medvedev et al. ($p$-$H_2$, 3.04 MPa) [50]

in Fig. 3, although the calculated densities do not agree with the experimental data. Hence, new PVT measurements at high temperatures and pressures are also desired. In this region of the surface of state, isobaric heat-capacity measurements are difficult. PVT data or speed of sound may do a better job of mapping the surface than isobaric heat capacity. Figure 8b shows the deviation of the EOS of Kunz et al., and the baseline is the EOS of Leachman for normal hydrogen. The deviation increases as temperature decreases below 50 K. There are not any experimental data for normal hydrogen to be compared, but speed-of-sound data below 50 K exist. The EOS of Leachman for normal hydrogen agrees well with the data as mentioned in the next section.

## 5.4 Speed of Sound

The representation of speed-of-sound experimental data for parahydrogen was much improved by the EOS of Leachman compared with that of Younglove. The comparisons of speed of sound with the EOSs of Leachman for parahydrogen and normal hydrogen are shown in Fig. 9. Speed of sound is also different between parahydrogen and normal hydrogen. The large difference is shown near 150 K as well as for the heat capacity, and the maximum deviation reaches approximately 4 % at 1 MPa and 7 %

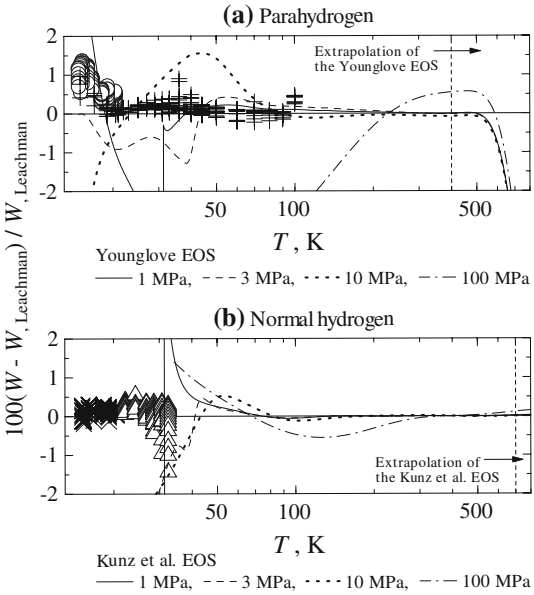


**Fig. 9** Deviations of speed of sound from the EOSs of Leachman [8] for **(a)** parahydrogen and **(b)** normal hydrogen: (○) van Itterbeek et al. ($p$-$H_2$) [53], (×) van Itterbeek et al. ($n$-$H_2$) [53], (+) Younglove ($p$-$H_2$) [54], (△) van Dael et al. ($n$-$H_2$) [55]

at 100 MPa. Figure 9a shows deviations of the experimental data of van Itterbeek et al. [53] up to 24 MPa, that of Younglove [54] up to 32 MPa, and the EOS of Younglove for parahydrogen. The baseline is the EOS of Leachman for parahydrogen. The EOS of Leachman for parahydrogen agrees with the experimental data of van Itterbeek et al. and Younglove within 1.5 %. The EOS of Younglove for parahydrogen is in good agreement with the EOS of Leachman for parahydrogen above 100 K although a large deviation is shown at 100 MPa. The EOS of Younglove does not represent the experimental data below 100 K well. Figure 9b shows deviations of the experimental data of van Itterbeek et al. [53] up to 23 MPa, that of van Dael et al. [55] up to 25 MPa, and the EOS of Kunz et al. from the EOS of Leachman for normal hydrogen. The EOS of Kunz et al. for normal hydrogen agrees with the EOS of Leachman for normal hydrogen for temperatures above 100 K. The deviation from the EOS of Leachman for normal hydrogen increases as temperature decreases below 50 K as well as for the isobaric heat capacity shown in Fig. 8b. For the speed of sound, the experimental data of van Itterbeek et al. and van Dael et al. for normal hydrogen exist, and the EOS of Leachman for normal hydrogen agrees well with the experimental data within 1.5 % except near the critical point.

## 6 Conclusions

Currently available EOSs for hydrogen were reviewed through comparisons of PVT, saturated properties, heat capacity, and speed of sound along with a summary of the data for the critical point, normal boiling point, and triple point. The Younglove EOS has been the leading formulation for over 25 years, but this EOS will be replaced

by the latest EOSs. The EOSs of Leachman for ortho-, para-, and normal hydrogen are recommended to calculate the thermodynamic properties with their critical points. Regarding the normal boiling points of parahydrogen and normal hydrogen, and the triple point of normal hydrogen, the recommended values by the CCT of BIPM are considered to be reliable. The triple point of parahydrogen is a fixed point of ITS-90. The EOSs of Leachman represent the existing experimental data most accurately and are useful for wide ranges of temperature and pressure. The proper use of the EOSs involves consideration of the differences of the saturated properties, heat capacity, and speed of sound among ortho-, para-, and normal hydrogen. Although the available temperature and pressure range of the EOS was extended recently, new accurate PVT measurements at high temperature and high pressure are desired as well as saturated-vapor-density and heat-capacity measurements at low temperatures.

**Acknowledgments** This research has been conducted as part of the "Fundamental Research Project on Advanced Hydrogen Science" funded by the New Energy and Industrial Technology Development Organization (NEDO). The authors thank Mr. Jacob Leachman of the University of Idaho for providing his master's thesis and also thank Dr. Marcia Huber of NIST for providing miniREFPROP. Finally, the authors thank Dr. Peter L. Woodfield for valuable discussions.

## References

1. A. Michels, M. Goudeket, Physica **8**, 347 (1941)
2. A. Michels, W. de Graaff, T. Wassenaar, J.M.H. Levelt, P. Louwerse, Physica **25**, 25 (1959)
3. B.A. Younglove, J. Phys. Chem. Ref. Data **11**, 1 (1982)
4. M. Jaeschke, A.E. Humphreys, *The GERG Databank of High Accuracy Compressibility Factor Measurements*, GERG Technical Monograph 4, Verlag des Vereins Deutscher Ingenieure, Düsseldorf, Germany (1990)
5. K. Matsuishi, E. Gregoryanz, H. Mao, R.J. Hemley, J. Chem. Phys. **118**, 10683 (2003)
6. R.T Jacobsen, J.W. Leachman, S.G. Penoncello, E.W. Lemmon, Int. J. Thermophys. **28**, 758 (2007)
7. J.W. Leachman, R.T Jacobsen, S.G. Penoncello, M.L. Huber, Int. J. Thermophys. **28**, 773 (2007)
8. J.W. Leachman, *Fundamental Equations of State for Parahydrogen, Normal Hydrogen, and Orthohydrogen*, Master's Thesis, University of Idaho (2007)
9. J.W. Leachman, R.T Jacobsen, S.G. Penoncello, E.W. Lemmon, J. Phys. Chem. Ref. Data **38**, 721 (2009)
10. O. Kunz, R. Klimeck, W. Wagner, M. Jaeschke, *The GERG-2004 Wide-Range Equation of State for Natural Gases and Other Mixtures*, GERG Technical Monograph 15 (2007)
11. N. Sakoda, K. Shindo, K. Shinzato, M. Kohno, Y. Takata, M. Fujii, in *Proceedings 29th Japan Symposium on Thermophysical Properties*, Tokyo, 2008, p. 402
12. H.W. Woolley, R.B. Scott, F.G. Brickwedde, J. Res. Natl. Bur. Stand. **41**, 379 (1948)
13. A. Michels, W. Graff, G.J. Wolkers, Appl. Sci. Res. A **12**, 9 (1963)
14. H.M. Roder, L.A. Weber, R.D. Goodwin, NBS Monograph 94 (1965)
15. R.D. McCarty, L.A. Weber, NBS Technical Note 617 (1972)
16. H.M. Roder, R.D. McCarty, W.J. Hall, NBS Technical Note 625 (1972)
17. R.D. McCarty, NBS Internal Report 74–357 (1974)
18. L.A. Weber, NASA-SP-3088 (1975)
19. H.M. Roder, R.D. McCarty, NBS Internal Report 75–814 (1975)
20. R.D. McCarty, NASA-SP-3089 (1975)
21. R.D. McCarty, NBS Technical Note 1025 (1980)
22. R.D. McCarty, J. Hord, H.M. Roder, NBS Monograph 168 (1981)
23. E. Bender, VDI-Forschungsheft **609**, 15 (1982)
24. A. Farkas, *Orthohydrogen, Parahydrogen and Heavy Hydrogen* (Cambridge University Press, Cambridge, 1935)
25. A.H. Larsen, F.E. Simon, C.A. Swenson, Rev. Sci. Instrum. **19**, 266 (1948)

26. R.D. Goodwin, D.E. Diller, H.M. Roder, L.A. Weber, J. Res. Natl. Bur. Stand. **67A**, 173 (1963)
27. D. White, A.S. Friedman, H.L. Johnston, J. Am. Chem. Soc. **72**, 3565 (1950)
28. H.J. Hoge, J.W. Lassiter, J. Res. Natl. Bur. Stand. **47**, 75 (1951)
29. H.M. Roder, D.E. Diller, L.A. Weber, R.D. Goodwin, Cryogenics **3**, 16 (1963)
30. W.H. Keesom, A. Bijl, H. van der Horst, Commun. Kamerlingh Onnes Lab. Univ. Leiden 217A, 1 (1931)
31. R.B. Scott, F.G. Brickwedde, H.C. Urey, M.H. Wahl, J. Chem. Phys. **2**, 454 (1934)
32. H.J. Hoge, R.D. Arnold, J. Res. Natl. Bur. Stand. **47**, 63 (1951)
33. E.R. Grilly, J. Am. Chem. Soc. **73**, 843 (1951)
34. L.A. Weber, D.E. Diller, H.M. Roder, R.D. Goodwin, Cryogenics **2**, 236 (1962)
35. C.R. Barber, A. Horsford, Br. J. Appl. Phys. **14**, 920 (1963)
36. A. van Itterbeek, O. Verbeke, F. Theewes, K. Staes, J. de Boelpaep, Physica **30**, 1238 (1964)
37. J. Ancsin, Metrologia **13**, 79 (1977)
38. R.C. Kemp, W.R. Kemp, Metrologia **15**, 155 (1979)
39. M.J. Hiza, Fluid Phase Equilib. **6**, 203 (1981)
40. R.E. Bedford, G. Bonnier, H. Maas, F. Pavese, Metrologia **33**, 133 (1996)
41. F. Henning, J. Otto, Phys. Z. **37**, 633 (1936)
42. A.R.H. Goodwin, K.N. Marsh, W.A. Wakeham, International Union of Pure and Applied Chemistry, Physical Chemistry Division, Commission on Thermodynamics (ed.), *Measurement of the Thermodynamic Properties of Single Phase* (Elsevier, Amsterdam, 2003), p. 23
43. NIST Chemistry WebBook, http://webbook.nist.gov/chemistry/
44. E.A. Amagat, Ann. Chim. Phys. **29**, 68 (1893)
45. D.S. Tsiklis, V.Ya Maslennikova, S.D. Gavrilov, A.N. Egorov, G.V. Timofeeva, Dokl. Akad. Nauk SSSR **220**, 1384 (1975)
46. D.H. Liebenberg, R.L. Mills, J.C. Bronson, Los Alamos National Laboratory Report No. LA-6641-MS (1977)
47. D.H. Liebenberg, R.L. Mills, J.C. Bronson, Los Alamos National Laboratory Report No. LA-6645-MS (1977)
48. D.C. Presnall, J. Geophys. Res. **74**, 6026 (1969)
49. R.D. Goodwin, D.E. Diller, H.M. Roder, L.A. Weber, Cryogenics **2**, 81 (1961)
50. V.A. Medvedev, Yu.A. Dedikov, M.P. Orlova, Russ. J. Phys. Chem. (Engl. Transl.) **45**, 297 (1971)
51. B.A. Younglove, D.E. Diller, Cryogenics **2**, 348 (1962)
52. M. Jaeschke, P. Schley, Int. J. Thermophys. **16**, 1381 (1995)
53. A. van Itterbeek, W. van Deal, A. Cops, Physica **29**, 965 (1963)
54. B.A. Younglove, J. Acoust. Soc. Am. **38**, 433 (1965)
55. W. van Dael, A. van Itterbeek, A. Cops, J. Theon, Cryogenics **5**, 207 (1965)
56. R. Wiebe, V.L. Gaddy, J. Am. Chem. Soc. **60**, 2300 (1938)
57. E.P. Bartlett, H.L. Cupples, T.H. Tremearne, J. Am. Chem. Soc. **50**, 1275 (1928)
58. J.G. Aston, E. Willihnganz, G.H. Messerly, J. Am. Chem. Soc. **57**, 1642 (1935)
59. R.B. Scott, F.G. Brickwedde, J. Chem. Phys. **5**, 736 (1937)
60. D. White, A.S. Friedman, H.L. Johnston, J. Am. Chem. Soc. **72**, 3927 (1950)